C. R. Acad. Sci. Paris, t. 1, Série II c, p. 567-575, 1998
Chimie organique physique/*Physical organic chemistry*

Rigid organic nanodisks of controlled size: A catanionic formulation

Monique DUBOIS [a]*, Thadeus GULIK-KRZYWICKI [b], Bruno DEMÉ [c], Thomas ZEMB [a]

[a] Service de chimie moléculaire, CEA/Saclay, Bât. 125, 91191 Gif-sur-Yvette cedex, France
E-mail: duboism@nanga.saclay.cea.fr
[b] C.G.M., 91190 Gif-sur-Yvette, France
[c] I.L.L., 38043 Grenoble, France

(Received 2 April 1998, accepted after revision 27 April 1998)

Abstract – We show that organic rigid nanodisks of controlled size can be produced using a balanced pair of ionic surfactant molecules in a catanionic system. The counter-ion for the cationic surfactant is hydroxide. The counter-ion of the anionic surfactant is the hydronium ion. Close to equimolarity, counter-ions from water molecules: fluid solutions of ultra-low conductivity are obtained. This solution contains rigid disks of thickness 4 nm: chains are frozen and surfaces are covered by ion pairs formed by the headgroups. The overall size of the disks is continuously adjustable from micrometer to nanometer size and is controlled by the excess of one of the two single chain surfactants involved. Unbound dispersed, nematic and lamellar structures are detected and located in the ternary equilibrium phase diagram at room temperature. © Académie des sciences/Elsevier, Paris

nanodisks / lamellar phase / catanionic surfactants

Résumé – Fabrication de nanodisques organiques rigides à l'aide d'un mélange catanionique de tensioactifs. Nous montrons que des nanoplaquettes rigides de taille contrôlable peuvent être obtenues en utilisant un mélange de tensioactifs catanioniques dont l'un porte un H^+, l'autre un hydroxyde. On obtient des solutions diluées isotropes optiquement et qui contiennent des nanodisques rigides d'épaisseur 4 nm. Les chaînes hydrocarbonées sont dans l'état cristallin. La taille des nanoplaquettes organiques formées est continûment ajustable, de l'ordre du micromètre à quelques nanomètres. Les plaquettes sont constituées d'une partie centrale plate et rigide. Des paires d'ions stabilisent chacune des faces. Un premier diagramme de phase d'équilibre schématique comprend des zones isotropes, nématiques et lamellaires. © Académie des sciences/Elsevier, Paris

nanodisques / phase lamellaire / surfactants catanioniques

Version française abrégée

Depuis les travaux d'Hoffmann et de Kaler, on sait que des mélanges de tensioactifs anioniques et cationiques en solution diluée peuvent produire des vésicules unilamellaires à l'équilibre thermodynamique.

Notre but est d'obtenir des systèmes colloïdaux fortement couplés, dans lesquels les interactions répulsives s'étendent plus loin que les premiers voisins.

Nous montrons que des nanoplaquettes rigides de taille contrôlable peuvent être obtenues en utilisant un mélange de tensioactifs catanioniques. Si le contre-ion du surfactant cationique est un hydroxyde alors que le contre-ion du partenaire anionique est un ion hydronium, des molécules d'eau

Communicated by Michel POUCHARD.

* Correspondence and reprints.

sont formées lors du mélange des tensioactifs. On obtient ainsi des solutions diluées isotropes optiquement et de conductivité remarquablement basse (de l'ordre de 100 $\mu S \cdot cm^{-1}$), ce qui démontre que les espèces ioniques dominantes sont en concentration de l'ordre de 10 $\mu mol \cdot L^{-1}$.

La solution colloïdale obtenue contient alors des nanodisques rigides d'épaisseur 4 nm. Les expériences de diffusion de rayons X aux angles moyens démontrent que les chaînes hydrocarbonées sont dans l'état cristallin à température ambiante : l'intérieur hydrophobe de la nanoplaquette est un cristal bidimensionnel de chaînes hydrocarbonées.

Le diamètre des nanoplaquettes organiques formées est continûment ajustable dans une gamme qui va de 3 µm à 30 nm. La distribution de tailles est déterminée par comptage sur des clichés de cryofracture. Les plaquettes sont constituées d'une partie centrale plate et rigide. Le comportement asymptotique mesuré aux très petits angles en diffusion de neutrons permet de fixer une limite inférieure pour la longueur de persistance dans le plan à 1 nm, à température ambiante et pour une épaisseur de 4 nm. Cela signifie que le module d'élasticité est de l'ordre de 0,2 GPa, une valeur exceptionnellement élevée pour un système moléculaire organisé constitué de molécules organiques.

Des paires d'ions stabilisent chacune des faces. Le bord des nanoplaquettes est constitué principalement du tensioactif ionique en excès : la courbure spontanée du tensioactif ionique forme une interface très courbée vers l'intérieur hydrophobe. La taille des nanoplaquettes est fixée principalement par chaque fraction molaire des composés anionique et cationique en présence. Lorsque le rapport molaire tend vers un, la charge électrique globale des nanodisques diminue et l'on produit les nanoplaquettes les plus grandes, car le coût en entropie de mélange nécessaire à former les bords des nanoplaquettes ne peut pas être compensé par le gain d'énergie d'interaction électrique entre plaquettes associé à la dispersion des charges.

Ces nanoplaquettes ont été rencontrées en phase isotrope où les plaquettes sont indépendantes, en phase nématique et en phase smectique. Un premier diagramme de phase d'équilibre schématique est déterminé. Les applications possibles des nanoplaquettes sont : l'orientation de molécules adsorbées sur des plaquettes dans la phase nématique diluée, orientable en champ magnétique et dans la polymérisation en surface des nanodisques de composés inorganiques. L'utilisation de nanodisques ultrarigides de catanioniques comme support réactionnel présente un avantage unique par rapport aux matrices cristal liquide actuellement utilisées : les nanodisques peuvent être tranformés en micelles, par ajout d'un excès de tensioactif cationique.

1. Introduction

Since the pioneering work of Hoffmann [1], it is known that mixtures of anionic and cationic surfactants – now labelled as catanionics – is a procedure capable of producing large aggregates of limited size. Limited rods and a nematic phase have been observed in the tetradecylpyridinium–heptylsulfonate–water system. The second crucial observation in the understanding of catanionic systems was the experimental evidencing of unilamellar vesicles at thermodynamic equilibrium by Kaler and coworkers [2]. For instance, by mixing sodium octylsulfate and acetyltrimethylammonium-bromide, cylindrical micelles coexist with closed unilamellar vesicles in the diluted region of the phase diagram [3]. At the maximum concentration of existence, these isotropic solutions are in equilibrium with a liquid crystal which is a concentrated lamellar phase. Khan and co-workers have systematically studied complete pseudo-ternary phase diagrams of several catanionic systems and recently elaborated an up-to-date review of the molecular systems yet explored [4].

In all these systems, two oppositely charged ionic surfactants are mixed. Excess salt is formed by liberation of the counter-ions. For a total surfactant concentration of about 20 g/L, this means that the ionic strength due to this added excess salt is of the order of 0.1 M, thus inducing a Debye screening length of the order of 0.3 nm. Indeed, strongly screened electrostatic interaction dominates the thermodynamic behavior of such catanionic systems containing five components (two surfactants, two counter-ions and water), bound by one electroneutrality constraint [5].

The aim of this work is to try to identify stability regions of 'true' catanionics, i.e. catanionic aggregates in the absence of residual counter-ions. If stable surfactant aggregates exist in low ionic strength conditions, for exam-

ple micromoles per liter, the electric coupling will be orders of magnitude higher than in classical catanionic solutions. These strongly coupled systems described here for the first time should have some common features with clay systems, such as diluted solutions of high osmotic pressure.

The method proposed here to avoid the presence of excess counter-ions is to use the mixture of an insoluble fatty acid (myristic acid) with a cationic surfactant ion exchanged in its hydroxide form. Since the two counterions react to form water and the cmc of the mixed system is of the order of ten micromoles per liter, this choice of catanionic components ensures that the Debye screening length is larger than the average interparticular distance, the condition of highly coupled electrostatic behavior of colloids.

The present paper demonstrates the presence of several microstructures of strongly coupled charged nanodisks: disks in equilibrium with micelles, disks in equilibrium with a swollen lamellar phase and unbound isotropic solution of disks.

2. Experimental

A classical method used for selecting a given counter-ion for an ionic surfactant is to use ion exchanging resin, such as BIO-RAD AG MP-1. The resin is first loaded to saturation with a concentrated NaOH 1 M solution. The column is then washed with 10 % ethanol solution in water to remove excess sodium ion. A concentrated surfactant (0.1 M with 10 % ethanol added) is then eluted through the column. The output of the column is evaporated under reduced pressure, redissolved in water and lyophilised. Applied four to five times to CTABr (cetyltrimethylammonium bromide), this procedure leaves in the final lyophilised surfactant 98.5 % of the desired (OH) counter-ion, but still of the order of 1.5 % of the initial bromide.

To obtain CTAOH with more 99.9 % ion exchanged, we have used an improved procedure. CTABr (0.1 M) is reacted in stoechiometric quantity with Ag_2O. Silver oxide powder gives silver hydroxide in solution Reaction produces insoluble silver bromide which is centrifuged twice (4000 rpm and then 20000 rpm twice during one night) to remove not only large colloidal precipitates, but also the AgBr nanoparticles. To avoid reaction with dissolved CO_2, the whole procedure has to be done using degassed water and under controlled nitrogen atmosphere in a glove box. Capillary electrophoresis is used to check the absence of residual parasitic counter-ions (less than 0.1 %) or residual bromide (less than 0.01 %).

The myristic acid was of commercial origin and used without further purification. Dosage using capillary electrophoresis could not evidence the presence of residual parasitic counterions coexisting with H^+: the highest possible value of residual parasitic counter-ions of our sample is estimated to 0.01 molar fraction versus carboxylate.

Cryofracture experiments were conducted in original sample or in the presence of 30 % glycerol and allows observation of swollen lamellar phase with the same method and precision than described for cationic lamellar phases and vesicles [6]. Small angle neutron scattering was performed at ILL on spectrometers D11 and D22 using standard data reduction procedures.

SAXS data were obtained on a standard Guinier–Mering camera for large angles ($0.04\ Å^{-1} < q < 2\ Å^{-1}$) and on a home build Huxley–Holmes type camera for low-q spectra ($0.015\ Å^{-1} < q < 0.4\ Å^{-1}$) [7]. Nature of the phase with rigid chains was determined by the method proposed by Tardieu and Luzzatti, using identification from the position, number and shape from reflections in the range of 4.2 Å Bragg spacing [8].

3. Results

Since there is no salt in excess, the two controlling variables are the volume fraction and the anionic mole fraction r:

$$r = [C_{13}COO^-]/([CTA^+]+[C_{13}COO^-])$$

We describe in this paper mainly the region $r < 0.5$, i.e. when the cationic surfactant is in excess, the surfactant aggregate is negative and the apparent pH measured by an electrode is higher than 7. The excess of counter-ions corresponds to the excess OH^- ions not neutralised by the fatty acid.

The existence of extraordinarily large surfactant aggregates is suspected from unusually strong light, X-ray and neutron scattering obtained in the diluted region of the phase diagram, i.e. when r is of the order of 0.40 and volume fraction of surfactant of the order of 1–2 %. Unlike the case of limited size vesicles [9], the SANS observed in the dilute range behaves as q^{-2} as shown of *figure 1*.

Since there is no inflexion point visible at q around 5.10^{-4} Å^{-1}, the in plane persistence length of platelets producing the scattering shown on *figure 1* exceeds 1 µm. From the Guinier plot for flat particles as shown in the insert, one deduces from the steep minimum position that the bilayer thickness is 43 ± 0.5 Å. From the SAXS peaks detected at high angles, we know that the chains are frozen at room temperature in the platelet, thus inducing a high stiffness of the bilayer. Near from the binary axis, in the quasi-binary CTAOH/water system ($r \rightarrow 0$), scattering intensity is lower and compatible with giant wormlike micelles [10].

Diluted samples with volume fraction of the order of 1 % were studied using electron microscopy. The disks observed in the diluted region are shown on *figure 2*. The characteristic sizes, obtained on the statistics of the order of 100 objects, are shown on *table I*.

Table I. Composition and known characteristics of the platelets of thickness 4.3 nm shown on *figure 2*.

Tableau I. Composition et caractéristiques des nanodisques d'épaisseur 4,3 nm de la *figure 2*.

A	r = 45.4 %	a = 2.5	D = 2600 ± 500 nm
B	r = 43,0 %	a = 1.8	D = 330 ± 120 nm
C	r = 41.6 %	a = 1.55	D = 80 ± 40 nm
D	r = 39.0 %	a = 1.1	D = 30 ± 5 nm

Total surfactant mass fraction c, molar fraction r, a area per charge in nm^2, D average diameter and median deviation obtained by measurement of 60 platelets on the TEM image.

Concentration massique c, rapport molaire r de tensioactif anionique, a aire moléculaire par charge structurale en nm^2, D diamètre moyen et écart médian obtenu par mesure de 60 objets.

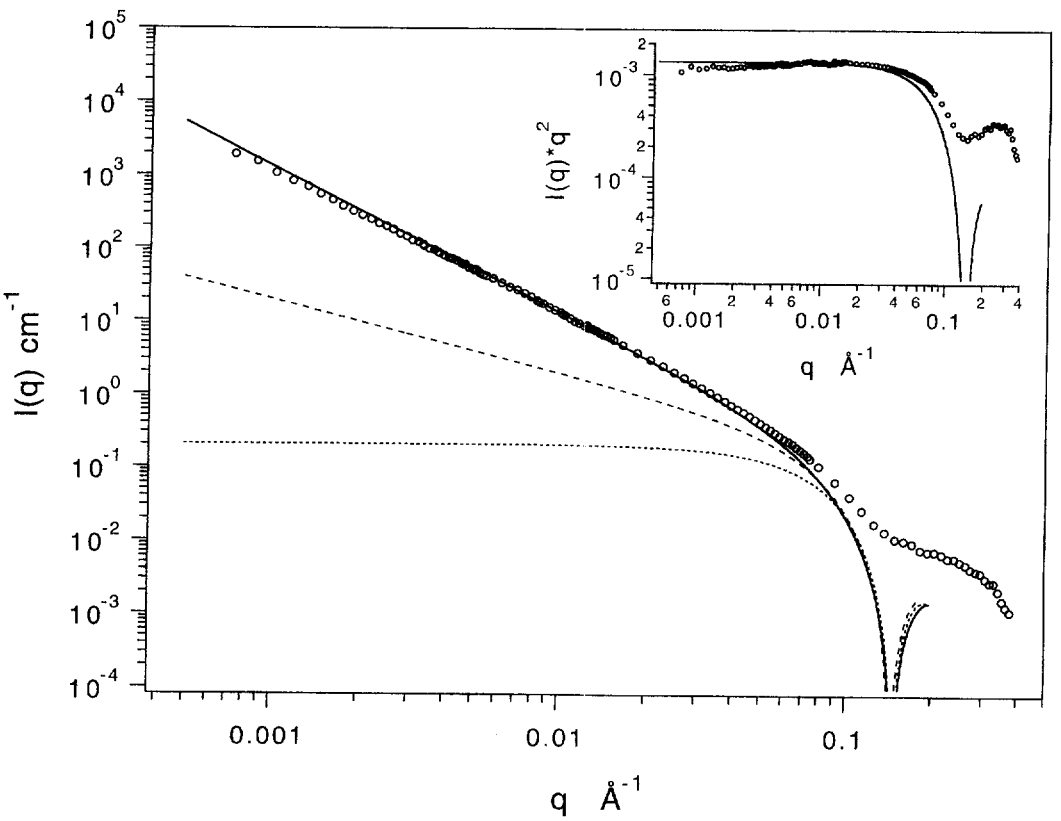

Figure 1. SANS produced by a diluted (c = 1.5 %) isotropic (U) dispersion of nanodisks. Due to the low structural charge, the structure factor can be neglected. The scattering observed is compared to the form factor of an infinite disk of thickness 4.26 nm. Form factors of spherical and cylindrical micelles presenting a first oscillation at the same q-value are shown for comparison.

Figure 1. Spectre de diffusion de neutrons d'une solution de nanodisques rigide peu chargée, le rapport molaire r = 45,7 % et la concentration 1,5 %. En raison de la faible charge structurale (a = 0,11 nm^2/q), le facteur de structure est négligeable. Le spectre est comparé au facteur de forme d'un disque plan infini d'épaisseur 4,26 nm. À titre de contre-exemple, les facteurs de forme de micelles sphériques et cylindriques présentant un premier minimum au même endroit que l'expérience sont tracés en pointillés à la même échelle.

In all of the samples imaged, the net surface charge is positive, due to the excess of cationic surfactant. Moreover, the equilibrium size is strongly dependant on the ratio between anionic and cationic surfactant: overall size shrinks from over a micron to 30 nm within a molar ratio change of less than 10 %.

The apparent pH, measured with an standard electrode, is close to 13 for all the samples: OH^- is the dominant counter-ion; its concentration is close to the excess of cationic surfactant for samples which are not in contact with atmospheric CO_2. The conductivity is also low, in the order of 100 microsiemens, demonstrating that there is no excess salt formed by residual parasitic counter-ions [10]. These sample contains only disks, without coexistence of spherical or giant flexible cylindrical micelles. This is shown on *figure 1*: we have superposed to the data the SANS spectra calculated for non-interacting micelles: these are orders of magnitude lower. Simulation on the insert gives bilayer thickness from the dip position as: 4.3 nm.

What is the mechanism of formation of these platelets which exist only in a narrow range of molar ratio between the two surfactants? A par-

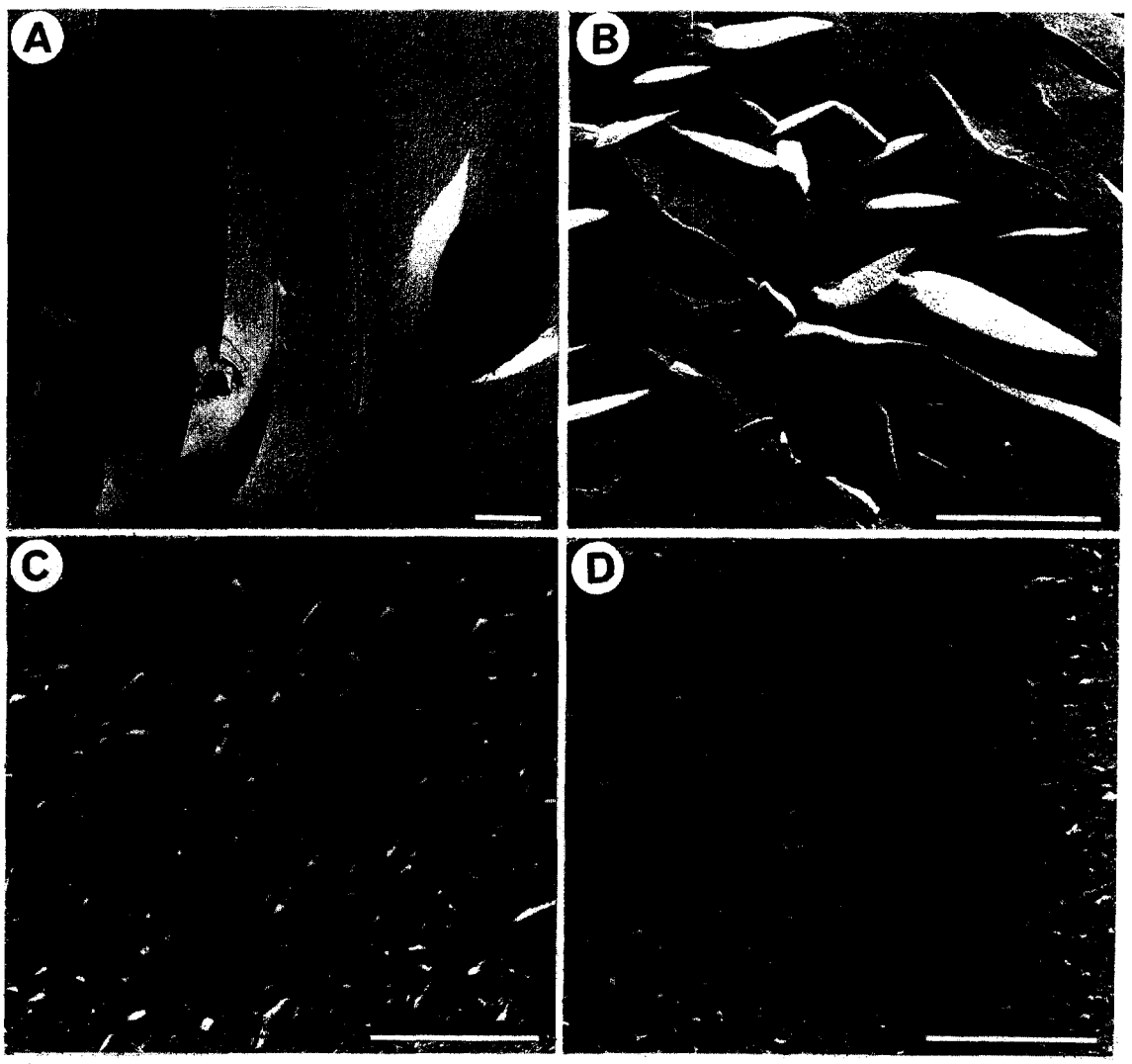

Figure 2. Cryoetching TEM images obtained from nanodisks in the diluted region of the phase diagram: (A) molar ratio R = 45.4 %, concentration (by weight) c = 0.17 %; (B) R = 43.0 %, c = 3 %; (C) R = 41.6 %, c = 3 % ; (D) R = 39.0 %, c = 3 %. From (A) to (D), the structural charge of nanodisks increases and the average diameter decreases.

Figure 2. Clichés de microscopie électronique d'échantillons obtenus par cryodécapage dans la zone diluée en eau. (A) Rapport molaire R = 45,4 %, concentration massique c = 0,17 % ; (B) R = 43,0 %, c = 3 % ; (C) R = 41,6 %, c = 3 % ; (D) R = 39,0 %, c = 3 %. De (A) à (D), la charge électrique nette négative des nanoplaquettes croît et la taille des nanodisques diminue.

tial molar separation between edges and faces is the driving force. Edges are enriched in anionic surfactants, while faces are an equimolar mixture of anionic and cationic surfactant. The reasons for this behavior are the following: (a) CTAOH with a low amount of myristic amount form cylindrical micelles ($r < 0.1$) found in the phase diagram; (b) size of platelets is increasing when approaching equimolarity, as it should because it is more and more difficult to form edges with high curvature (c) charged edges produce a strong scattering peak in concentrated samples ($c > 2\ \%$) while ion pair formation on the faces of nanodisks induces freezing of the hydrocarbon chains [10].

The driving mechanism is therefore a competition between local deviation from average concentration, at an entropy cost versus electrostatic energy, focused on edges kin the absence of salt [11]. The mechanism is close to the driving force for vesicle formation in catanionics mixtures with high salt content, where mixing entropy competes with bending energy as demonstrated by Safran [12, 13]. Spontaneous vesicles have already been evidenced in pure double chain hydroxide surfactants, binary analogs of the systems described here. The difference is that the chains are not frozen, therefore vesicles are formed [14]. In catanionic systems with fluid chains, the free energy terms involved in this competition have been calculated and compared to the position of the lamellar phase in the composition triangle [15].

Figure 3 shows scattering spectra obtained on the phases on equilibrium with platelets. L_β is a lamellar phase with frozen hydrocarbon chains. This lamellar phase swells up to 200 Å periodicity in the absence of dissolved CO_2 and more than 1000 Å in the presence of dissolved CO_2. The mechanism for that increased stability range is adsorption of carbonate ion on the globally neutral faces of the platelet. Bragg peaks remain sharp; to our knowledge periodicities exceeding 600 Å for some compositions with still 7 Bragg orders visible on a log scale are the highest values ever evidenced by SANS experiments for a swollen L_β gel. Extreme swelling of DMPC bilayers exceeding 1000 Å usually require addition of a sterically stabilizing polymer, such as a hydrophically modified polysaccharide [16].

In the diluted region around $r = 40\ \%$ with an overall concentration of 2 %, an isotropic to nematic transition takes place. After gentle centrifugation, the sample phase separates between an isotropic supernatant, which is a diluted solution of positively charged uncorrelated nanodisks. We label this phase by U^+. This isotropic liquid phase separates with a birefringence nematic phase of disks. The SANS spectra of this nematic phase N^+ is shown on *figure* 3. This nematic phase is often in coexistence of microphase separated domains of U^+ phases: this produces the strong increase of the scattering at low angle. We denominate by $[N^+]$ these biphasic samples. This coexistence of nematic and isotropic phase of colloids has been predicted by Marcelja and Ninham twenty years ago [17].

The apparition of a closed vesicles has nether been observed when cationic surfactant is in excess: this is due to the high bending rigidity of the bilayers, induced by the microcristalline nature of the frozen hydrocarbon chains.

Diluted regime of nanodisks represents a new structure in surfactant self-assembly. We have shown here proofs using scattering and electron microscopy of the existence of nanodisks of limited and controlled size. In the literature, a similar example exists. This microstructure of limited size, where ionic surfactants form the charged edges of a rigid disk without charges on the faces has been recently inferred from orientation of the molecules observed in a magnetic field applied on a diluted solution DMPC/DHPC [18]. The only experimental proof is NMR peak splitting and the faces are uncharged, due to the zwitterionic nature of DMPC. We are convinced that the finite platelet structure described by Vold as 'ideal bicelle' really exists as thermodynamic state of mixed surfactant self-assembly.

The phase diagram for the pure system and the system in contact with dissolved CO_2 plus some residual conterion bromide is shown on *figure* 4. A part of pure isotropic, nematic and lamellar phases, some biphasic regions have been identified after systematic investigation of the composition in the water corner of the phase triangle:

– nanodisks in equilibrium with a concentrated lamellar phase of periodicity of about 40 Å;

– lamellar phase in equilibrium with cylindrical flexible giant micelles;

– nematic phase in equilibrium with a diluted solution of nanodisks.

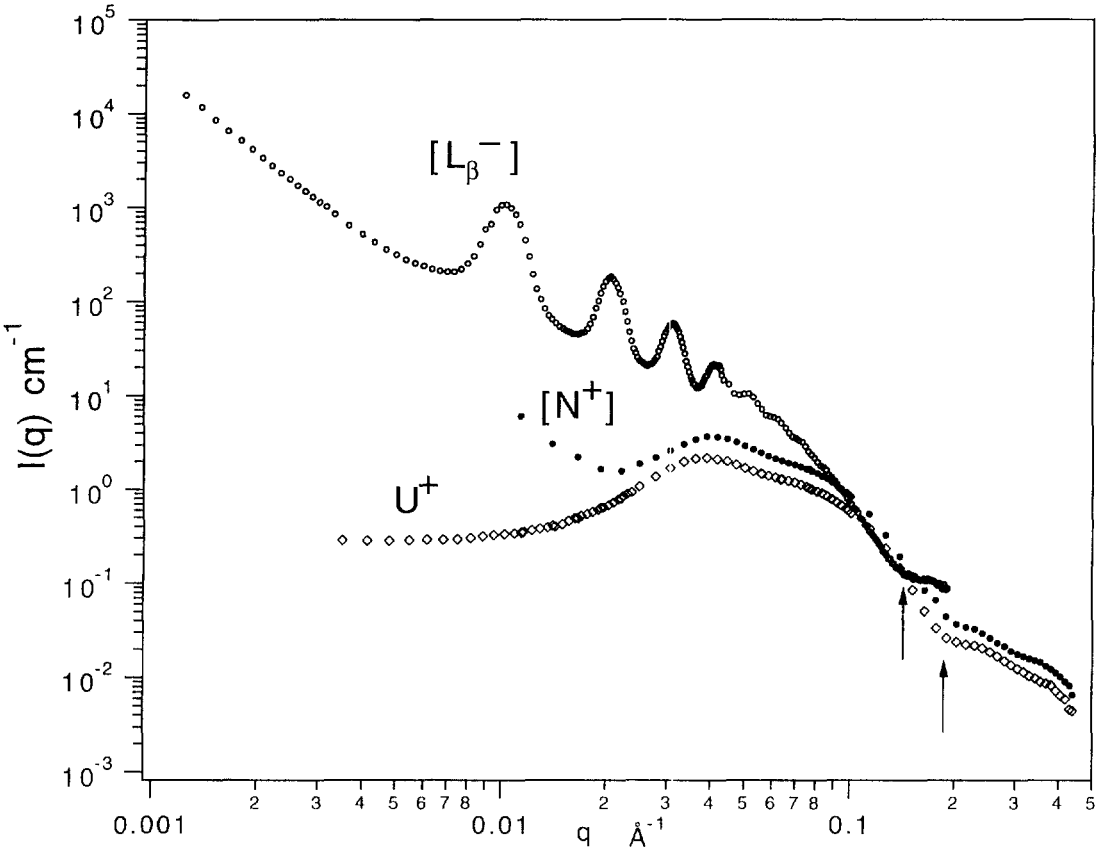

Figure 3. SANS (in log scale) produced by:
– a diluted lamellar phase of negatively charged nanodisks (r = 50.2 %, c = 3 %); seven diffraction peaks can be observed; the strong q^{-3} increase at low angle is the sign of a microphase separation occuring in the smectic bulk [L_β^-];
– a sample of initial composition (r = 34 %, c = 1.96 %), who has macroscopically phase separated in two fluids. The concentrated phase is a nematic phase of positively charged nanodisks ([N^+]). The diluted phase is an optically isotropic phase of unbound nanodisks (U^+).

Figure 3. Spectres de diffusion de neutrons en échelle logarithmique :
– d'une phase lamellaire diluée de nanodisques chargés négativement (r = 50,2 %, c = 3 %) ; sept ordres de diffraction sont observés ; la remontée aux petits angles est le signe d'une séparation en microphases [L_β^-].
– d'un échantillon de composition initiale (r = 34 %, c = 1,96 %) ayant démixé en une phase de disques cationiques en phase nématique ([N^+]) et une phase de disques isotropes (U^+). La phase nématique présente une séparation en microphases.

4. Discussion

Since the discovery of the linear swelling of the sponge phase [19, 20] and reverse sponge phase [21], which have been demonstrated to be connected structures, isolated disconnected platelet structure have been proposed, for example by Hoffmann. these platelets of fixed size were produced under shear from a catanionic gel P_β phase [22]. These objects but not directly observed as adjustable size isolated flat disks directly evidenced by electron microscopy.

These disks are extraordinarly rigid objects. From the microscopy pictures and undetectable in-plane correlation length, we evaluate a bending radius of 1/H = 3 µm for isolated platelets of size l = 0.3 µm and thickness d = 4.3 nm. The Young bending elasticity modulus Y can be derived from the bending elasticity F_b using:

$$F_b = 1/2\ Y\ (d^3.l^2/3)\ H^2 = 1/2\ K_c.\ H^2$$

Where K_c is the molecular film bending constant. At thermal equilibrium, equipartition theorem assigns an energy of $F_b = 1/2kT = 4.10^{-20}$ J to the bending mode of length l of the disk. The Young elasticity modulus is therefore 2.10^8 Pa for platelets, corresponding to K_c = 500 kT, twenty times larger than values reported for phospholipids with frozen chains.

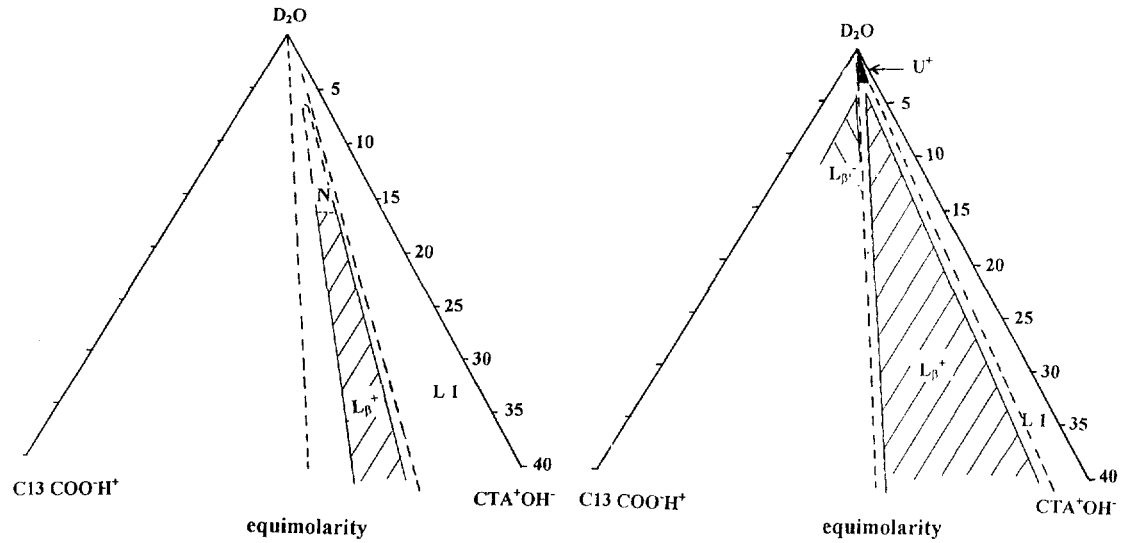

Figure 4. Schematic equilibrium phase diagram showing the relative location of the four structures described in this work:
– U is the diluted solution of unbound nanodisks,
– N^+ is the nematic phase of positively charged objects,
– L_β^+ is the lamellar phase of positively charged bilayers made with frozen chains,
– L_1 is the isotropic solution of giant micelles obtained when CTAOH is overwhelming.

Figure 4. Diagramme de phase d'équilibre schématique indiquant la localisation relative des quatre structures rencontrées dans la partie du diagramme riche en tensioactif cationique :
– U est la phase isotrope de nanodisques en solution diluée,
– N^+ est la phase nématique d'objets chargés positivement,
– L_β^+ est la phase lamellaire à chaînes rigides,
– L_1 est la solution isotrope de micelles géantes flexibles observées quand l'hydroxide de cétyltriméthylammonium est très majoritaire.

This unique high value of bending elasticity, even higher than rigidity of crystalline material such as clay, originates from the alternated charge network on present on the faces of nanodisks.

5. Conclusion

The new microstructure in surfactant self-assembly described here can have several uses as a colloidal dispersion media:

(a) The diluted nematic phase of stiff disks can be used to orient adsorbed molecules, in order to allow direct determination of coupling constants from NMR shifts, a new technique recently proposed for structural investigation of oligopeptides by liquid state NMR [23].

(b) These platelets could be used as a template for inorganic polymerization. For example, silica polymerisation in the form of nanometric lamellae has been made with infinite bilayers of pure cationic surfactants [24]. Using nanodisks, finite flat silica platelets could be produced by coating of catanionic nanodisks.

Finally, this model system of disks of known structural charge on edges, controlled size, and globally neutral charges should have some common and some distinctive features with clay platelets. The main difference is that catanionic diks are charged on the edges, as opposite to clay particles. If a simple procedure for evaluating osmotic pressure in the presence of single chain surfactants become available [25], the sensitivity of the osmotic pressure in this highly charged system upon the addition of small quantity of salt to this system could be very sensitive tool to test the prediction of modern theories of dispersion forces between added ions and the neutral faces of the nanodisks [26].

Acknowledgements

J.-Cl. Dedieu is acknowledged for realizing the cryofracture replica and photographs. P. Lixon is acknowledged for his especially efficient help and expertise in capillary electrophoresis.

References

[1] Hoffmann H., Kalus J., Schwander B., Ber. Bunsenges. Phys. Chem. 91 (1987) 99–106.

[2] Kaler E.W., Murthy A.K., Rodriguez B.E., Zasadzinski J.A., Science 245 (1989) 1371–1375.

[3] Yatcilla M.T., Herrington K.L., Brasher L.L., Kaler E.W., Chirovolu S., Zasadzinski J.A., J. Phys. Chem. 100 (1996) 5874–5879.

[4] Khan A., Marquès E., Catanionic surfactants, in: Robb I.D. (Ed.), Specialist Surfactants, Chapman et Hall, Glasgow, 1996, chapter III, p. 37.

[5] Bergström M., Langmuir 12 (1996) 2454–2463.

[6] Dubois M., Zemb T., Langmuir 7 (1991) 1352–1360.

[7] Le Flanchec V., Gazeau D., Taboury J., Zemb T., J. Appl. Crystallogr. 29 (2) (1996) 110–117.

[8] Tardieu A., Luzzati V., Reman F.C., J. Mol. Biol. 75 (1973) 711–733.

[9] Brasher L.L., Kaler E.W., Langmuir, 12 (1996) 6270–6276

[10] Zemb T., Dubois M., Demé B., Gulik-Krzywicki T., Science (1998) submitted.

[11] Fogden A., Daicic J., Mitchell D.J., Ninham B.W., Physica A 234 (1996) 167–188.

[12] Safran S.A. MacKintosh F.C., Pincus P.A., Andelman D.A, Science 248 (1990) 354–356.

[13] Safran S.A., MacKintosh F.C., Pincus P.A., Andelman D.A., Phys. Rev. A 43 (1991) 1071–1078.

[14] Ninham B.W., Evans D.F., Wei G.F., J. Phys. Chem. 87 (24) (1983) 5020–5025.

[15] Jokela P., Joensson B., Eichmueller B., Fontell K., Langmuir 4 (1988) 187–192.

[16] Demé B., Dubois M., Zemb T., Cabane B., Colloids Surfaces A 121 (1997) 135–143.

[17] Forsyth P.A., Marcelja S., Mitchell D.J., Ninham B.W., J. Chem. Soc., Faraday Trans. II 73 (1977) 84–88.

[18] Vold R., Prosser R., J. Mag. Res. B 113 (1996) 267–271.

[19] Ekwall P., Mandell L., Kolloid-Z und Zeitschrift für Polymere 233 (1968) 938.

[20] Ekwall P., Fontell K., Colloid Polym. Sci 266 (1988) 184–191, 267 (1988) 607–621.

[21] Warr G.G., Zemb T., Barnes I.S., Proc. 2nd World Surfactant Congress, Paris (mai 1988), ASPA 1 1988, pp. 368–376.

[22] Tamori K., Kihara K., Sanda H., Esumi K., Meguro K., Thunig C., Hoffmann H., Colloid Polym. Sci. 270 (1992) 885–893

[23] Tjandra N., Bax A., Science 278 (1997) 1111–1114.

[24] Dubois M., Cabane B., Langmuir 10 (1994) 1615–1617.

[25] Bagger-Joergensen H., Olsson U., Langmuir 12 (1996) 4057–4059.

[26] Ninham B.W., Langmuir 13 (1997) 2097–2108.